






The guanine nucleotide exchange factor VAV3 participates in ERBB4-mediated cancer cell migration

Received for publication, September 4, 2019, and in revised form, June 6, 2020. Published, Papers in Press, June 19, 2020. DOI 10.1074/jbc.RA119.010925

Veera K. Ojala^{1,2,3} , Anna M. Knittle¹, Peppi Kirjalainen^{1,2}, Johannes A. M. Merilahti^{1,2,3} , Maarit Kortesoja¹, Denis Tvorogov¹ , Katri Vaparanta^{1,2,3} , Shujun Lin⁴, Jürgen Kast⁴, Arto T. Pulliainen¹ , Kari J. Kurppa¹, and Klaus Elenius^{1,2,5,*} 

From the ¹Institute of Biomedicine and Medicity Research Laboratories and the ³Turku Doctoral Programme of Molecular Medicine, University of Turku, Turku, Finland, the ²Turku Bioscience Centre, University of Turku and Åbo Akademi University, Turku, Finland, the ⁴Biomedical Research Centre, Department of Chemistry, and Centre for Blood Research, University of British Columbia, Vancouver, British Columbia, Canada, and the ⁵Department of Oncology and Radiotherapy, Turku University Hospital, Turku, Finland

Edited by Alex Toker

ERBB4 is a member of the epidermal growth factor receptor (EGFR)/ERBB subfamily of receptor tyrosine kinases that regulates cellular processes including proliferation, migration, and survival. ERBB4 signaling is involved in embryogenesis and homeostasis of healthy adult tissues, but also in human pathologies such as cancer, neurological disorders, and cardiovascular diseases. Here, an MS-based analysis revealed the Vav guanine nucleotide exchange factor 3 (VAV3), an activator of Rho family GTPases, as a critical ERBB4-interacting protein in breast cancer cells. We confirmed the ERBB4–VAV3 interaction by targeted MS and coimmunoprecipitation experiments and further defined it by demonstrating that kinase activity and Tyr-1022 and Tyr-1162 of ERBB4, as well as the intact phosphotyrosine-interacting SH2 domain of VAV3, are necessary for this interaction. We found that ERBB4 stimulates tyrosine phosphorylation of the VAV3 activation domain, known to be required for guanine nucleotide exchange factor (GEF) activity of VAV proteins. In addition to VAV3, the other members of the VAV family, VAV1 and VAV2, also coprecipitated with ERBB4. Analyses of the effects of overexpression of dominant-negative VAV3 constructs or shRNA-mediated down-regulation of VAV3 expression in breast cancer cells indicated that active VAV3 is involved in ERBB4-stimulated cell migration. These results define the VAV GEFs as effectors of ERBB4 activity in a signaling pathway relevant for cancer cell migration.

ERBB receptors form the epidermal growth factor receptor (EGFR)/ERBB subfamily of receptor tyrosine kinases (RTK) that includes EGFR/ERBB1, ERBB2, ERBB3, and ERBB4. ERBB receptors are activated by the binding of EGF-like growth factors and transmit the growth factor signal into the activation of intracellular signaling cascades, such as mitogen-activated pro-

tein kinase and phosphoinositol 3-kinase (PI3K) pathways. Through these phosphorylation-dependent signaling cascades ERBB receptors regulate proliferation, differentiation, migration, and survival and play essential roles in embryogenesis and homeostasis of adult tissues. Abnormal ERBB signaling is a common feature of human pathologies such as cancer, neurological disorders, and cardiovascular diseases (1).

ERBB4 is expressed as four isoforms that are generated by alternative mRNA splicing. Two of the isoforms differ structurally in the extracellular juxtamembrane region (JM-a and JM-b), and two differ in the intracellular cytoplasmic domain (CYT-1 and CYT-2). The JM-a isoform, but not the JM-b, includes a sequence with a cleavage site for tumor necrosis factor- α -converting enzyme (TACE). TACE cleavage triggers a second cleavage by γ -secretase complex, releasing ERBB4 intracellular domain (ICD) into the cytosol (2–4). The CYT-1 isoform, but not the CYT-2 isoform, includes a short sequence that contains binding sites for the P85 subunit of PI3K (5) and WW domain-containing proteins (6, 7). Whereas the JM-a isoform is mostly expressed in epithelial tissues (such as those in the mammary gland and kidney) and the expression of JM-b is limited to mesenchymal tissues (such as heart and skeletal muscle), both CYT isoforms are usually expressed in the same cell types (8). ERBB4 is also expressed in several cancer types, and both increased and decreased expression compared with non-neoplastic control tissue have been reported (9).

The presence of isoforms diversifies the signaling mechanisms of ERBB4. Indeed, some ERBB4 functions are known to be isoform-specific. Unlike CYT-2, the CYT-1 isoform, which couples with PI3K, promotes chemotaxis and lamellipodia formation in fibroblasts in a PI3K-dependent manner (10). Interactions of ERBB4 with WW domain-containing E3 ubiquitin ligases are also specific to CYT-1, making it less stable than CYT-2 (6, 7). In addition to being more stable, the CYT-2 isoform is phosphorylated to a greater extent and has higher autokinase activity compared with CYT-1 (11, 12). Indeed, only the JM-a CYT-2 isoform promotes the survival of myeloid cells (11). Similar to cytoplasmic isoforms, JM-a and JM-b isoforms have been shown to promote distinct functions in different cell types (11, 13). Some of these functions can be mechanistically attributed to the soluble ICD released from the JM-a isoform.

This article contains [supporting information](#).

* For correspondence: Klaus Elenius, klaus.elenius@utu.fi.

Present address for Maarit Kortesoja: Drug Research Program, Division of Pharmaceutical Biosciences, Faculty of Pharmacy, University of Helsinki, Helsinki, Finland.

Present address for Denis Tvorogov: The Centre for Cancer Biology, SA Pathology and the University of South Australia, Adelaide, South Australia, Australia.

Present address for Jürgen Kast: Protagen Protein Services GmbH, Heilbronn, Germany.

ERBB4-VAV3 interaction

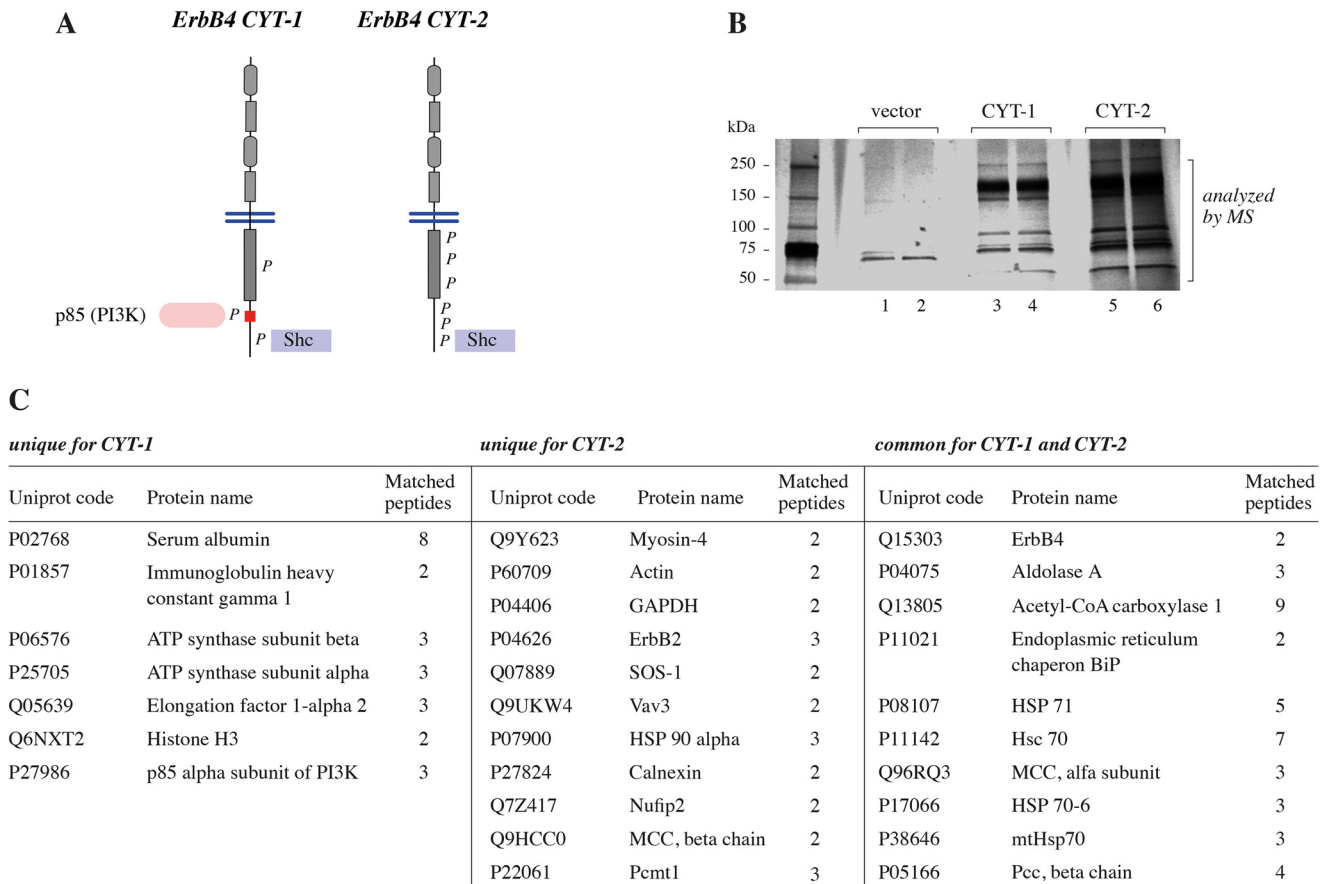


Figure 1. A, schematic structure of the ERBB4 isoforms JM-a CYT-1 and JM-a CYT-2. P, phosphorylated tyrosine residues in the cytoplasmic domains of activated ERBB4 isoforms. Red color in the CYT-1 cytoplasmic tail indicates the CYT-1-specific 16-amino acid insert. Whereas both isoforms have binding sites for Shc, the CYT-1-specific region has a binding site for P85, the regulatory subunit of PI3K. CYT-2 is more heavily phosphorylated than CYT-1. B, Strep-tagged ERBB4 JM-a CYT-1 and ERBB4 JM-a CYT-2 were expressed in MCF-7 cells, and the interacting proteins were purified using Strep-Tactin Superflow columns. The purified proteins were separated by SDS-PAGE and silver-stained. Each sample was loaded into two adjacent lanes of the gel. C, proteins copurifying with ERBB4 isoforms.

ERBB4 ICD is an active tyrosine kinase (14) that can translocate into the nucleus (4), where it regulates transcription (15, 16).

To characterize novel molecular components of ERBB4 signaling, we copurified ERBB4 JM-a CYT-1 and JM-a CYT-2–associating proteins from breast cancer cells and analyzed them by MS. Novel ERBB4-associating proteins included VAV3, a guanine nucleotide exchange factor (GEF) for Rho GTPases, whose activity modulates cell adhesion and motility (17, 18). Intriguingly, VAV proteins contain phosphotyrosine-binding Src homology 2 (SH2) domains, and the VAV GEF activity requires tyrosine phosphorylation of their activation domain by kinases, including RTKs (17, 19). We confirmed the ERBB4-VAV3 interaction by targeted MS and coimmunoprecipitation experiments, showed that ERBB4 stimulates tyrosine phosphorylation of the VAV3 activation domain, and demonstrated that VAV3 is involved in ERBB4-stimulated migration. These findings indicate that VAV GTPases are novel effectors of ERBB4 activity in a signaling pathway relevant for cancer cell migration.

Results

Proteomics identifies novel interaction partners of ERBB4

To identify novel ERBB4-interacting proteins, Strep-tagged ERBB4 constructs encoding the cleavable JM-a isoform of the

CYT-1 or CYT-2 type were generated and stably transfected to MCF-7 breast cancer cells (Fig. 1A). Cells were lysed, and the lysates were subjected to Strep purification to pull down Strep-tagged ERBB4 and coprecipitating proteins. Strep-tactin precipitates were analyzed by SDS-PAGE and silver staining (Fig. 1B) followed by MS to identify proteins present in the precipitates. MS identified several proteins that copurified with Strep-tactin in ERBB4-expressing lysates, but not in lysates of vector control cells (Table S1). Whereas 10 of the ERBB4-copurifying proteins were detected in both CYT-1 and CYT-2 samples, 7 proteins were specifically identified in CYT-1 samples and 11 in CYT-2 samples (Fig. 1C). One of the proteins copurifying only with ERBB4 CYT-1 was phosphatidylinositol-3-kinase regulatory subunit α (P85A), which is known to interact with CYT-1 but not with the CYT-2 isoform (Fig. 1C) (5). On the contrary, two signaling proteins known to associate with ERBB signaling complexes, ERBB2 and SOS1 (20, 21), were detected in ERBB4 CYT-2 samples only (Fig. 1C). These data suggest that cytoplasmic ERBB4 isoforms have specific and shared interaction partners.

Novel ERBB4 CYT-2–associating proteins included VAV3 (Fig. 1C), a guanine nucleotide exchange factor (GEF) for Rho GTPases (17). As previous studies have identified certain RTKs as activators of VAV-mediated signaling (19), we

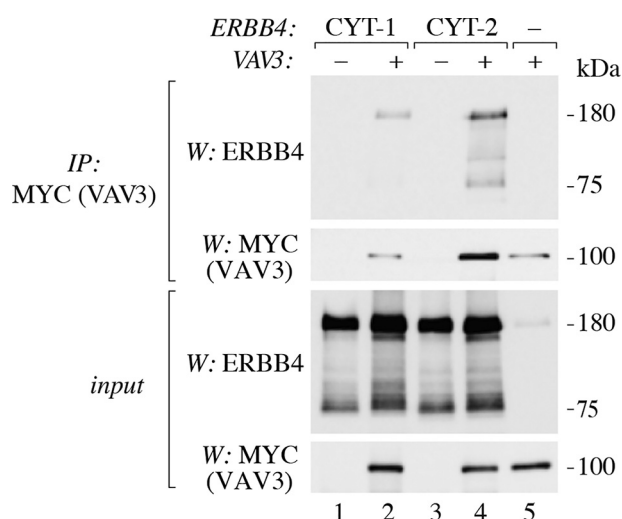


Figure 2. Interaction of ERBB4 isoforms with VAV3. COS-7 cells were transfected with constructs encoding ERBB4 JM-a CYT-1 or ERBB4 JM-a CYT-2 and MYC-HIS-tagged VAV3. Lysates were incubated with anti-MYC (2272) to immunoprecipitate (IP) VAV3. Immunoprecipitation samples and total lysates were analyzed by Western blotting (W) with anti-ERBB4 (E200) and anti-MYC (2272).

set to further validate and characterize the detected ERBB4-VAV3 interaction.

Validation of the ERBB4-VAV3 interaction by targeted proteomics

The MS data indicating a physical association of ERBB4 with VAV3 was controlled in a setting of endogenously expressed proteins. To this end, parental MCF-7 cells endogenously expressing moderate levels of both the JM-a CYT-1 and JM-a CYT-2 isoforms of ERBB4 (11) were stimulated or not with the ERBB4 ligand neuregulin-1 (NRG-1), and material coprecipitating with the endogenous ERBB4 was analyzed by VAV3-targeted MS. ERBB4 expression and ligand-induced ERBB4 phosphorylation were demonstrated by Western analyses (Fig. S1A). Targeted MS confirmed the interaction between endogenously expressed proteins and indicated that VAV3 peptides were more abundant in NRG-1-treated samples (Fig. S1B), suggesting that ERBB4 activation promoted the ERBB4-VAV3 interaction.

Characterization of the ERBB4-VAV3 interaction

To further validate the ERBB4-VAV3 interaction, a series of coimmunoprecipitation assays was carried out. First, MYC-HIS-tagged VAV3 was transiently expressed in COS-7 cells together with constructs encoding JM-a CYT-1 or JM-a CYT-2 isoforms of ERBB4 (Fig. 2). Cell lysates were incubated with anti-ERBB4 antibody to immunoprecipitate ERBB4-interacting proteins, and the precipitates were analyzed by Western blotting. The interaction of ERBB4 CYT-2 and VAV3 was readily detected (Fig. 2, lane 4), confirming the results of MS. VAV3 also interacted with transiently expressed ERBB4 CYT-1 (Fig. 2, lane 2).

In addition to full-length, ~180-kDa ERBB4 receptor, the ~75-kDa ERBB4 fragment (representing the ICD produced by proteolysis from the full-length receptor (3, 4)) was also

detected in coimmunoprecipitation assays (Fig. 2). As the detected 75-kDa ERBB4 could represent either the TACE-processed receptor fragment still attached to the cell membrane or the soluble ICD released from the membrane by γ -secretase, a coimmunoprecipitation experiment employing a construct encoding only the ICD fragment of ERBB4 was carried out. Interaction of the ERBB4 ICD and VAV3 was again readily detected, indicating that the soluble ICD is sufficient to mediate the ERBB4-VAV3 interaction (Fig. 3A, lane 2).

VAV proteins have been shown to interact with activated protein tyrosine kinases with their SH2 domains (17, 22). Indeed, substitution of arginine 697 to leucine (previously shown to be required for the integrity of the VAV3 SH2 domain (23)), as well as deletion of the VAV3 SH2 domain (using a construct named 1-PH (23)), abolished the interaction of ERBB4 and VAV3 in coimmunoprecipitation assays (Fig. 3, A and B), indicating that the ERBB4-VAV3 interaction was SH2 domain-dependent. Similar results were obtained when the soluble ERBB4 ICD was expressed instead of full-length ERBB4 receptor (Fig. 3A). In agreement with the phosphotyrosine-binding function of SH2 domains, a kinase-dead ERBB4 construct that is not tyrosine-phosphorylated (K751R (12)) did not interact with VAV3 (Fig. 3C and Fig. S2A).

Next, we set to determine the ERBB4 tyrosine residue(s) required for the interaction. The association of ERBB4 phosphopeptides with different SH2 domains has been analyzed in two studies. Kaushansky *et al.* (24) detected interactions of ERBB4 Tyr-1162- and Tyr-1258-containing phosphopeptides with the SH2 domain of a VAV family member, VAV2. Hause *et al.* (25) detected potential interactions of ERBB4 Tyr-1022, -1150, -1162, and -1258 with the VAV1 SH2 domain, ERBB4 Tyr-1208 with the VAV2 domain, and ERBB4 Tyr-1150 and -1202 with the VAV3 SH2 domain. To determine the role of these tyrosines in mediating the ERBB4-VAV3 interaction, tyrosine-to-phenylalanine mutant ERBB4 constructs were generated and analyzed for their ability to interact with VAV3 in a series of coimmunoprecipitation assays. Both Y1022F and Y1162F mutations disrupted the efficient interaction detected between WT ERBB4 and VAV3, indicating that these ERBB4 tyrosines were required for VAV3 docking (Fig. 3D). However, the interaction of ERBB4 Y1208F (Fig. S2A), Y1258F (Fig. S2A), and Y1202F (Fig. S2B) with VAV3 was comparable with that of WT ERBB4, demonstrating that these ERBB4 tyrosines were not necessary for the interaction. Together, these data validate the ERBB4-VAV3 interaction detected in the MS analyses of ERBB4-copurifying proteins and demonstrate that the interaction requires the SH2 domain of VAV3 as well as ERBB4 phosphotyrosines 1022 and 1162.

ERBB4 interacts with VAV1, VAV2, and VAV3

Three VAV genes (VAV1, VAV2, and VAV3) form the human VAV family (17). All VAV proteins have a highly similar structure, including a conserved SH2 domain (17). To study the putative interactions of ERBB4 with VAV1 and VAV2 in addition to VAV3, COS-7 cells were transfected with HA-tagged VAV proteins together with MYC-tagged ERBB4 JM-a CYT-2, and lysates were subjected to immunoprecipitation with anti-

ERBB4-VAV3 interaction

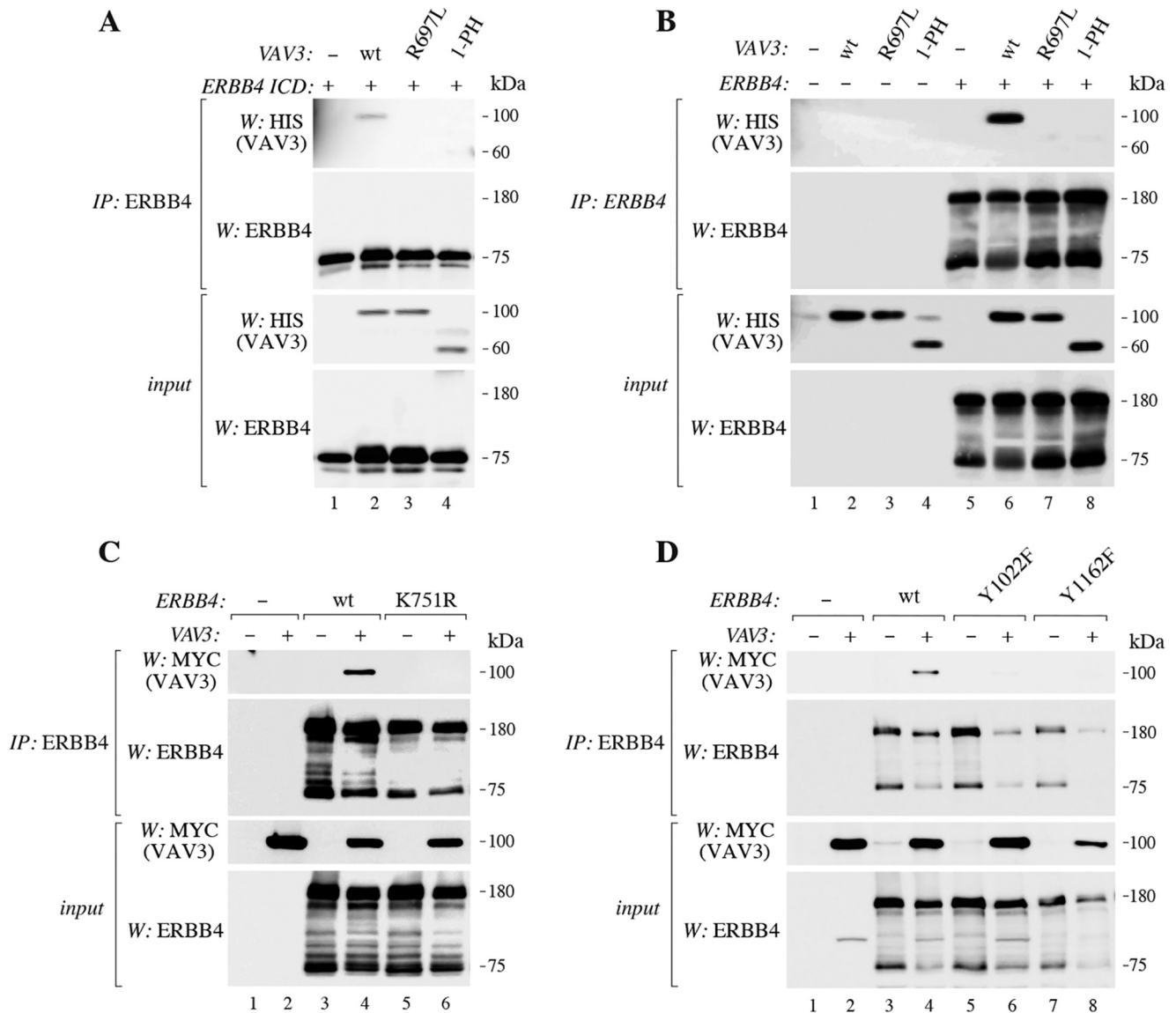


Figure 3. Molecular determinants of ERBB4-VAV3 interaction. *A*, COS-7 cells were transfected with ERBB4 (JM-a CYT-2 isoform) and WT or mutant MYC-HIS-tagged VAV3 constructs. Lysates were immunoprecipitated with anti-ERBB4 (sc-283). Immunoprecipitation (IP) samples and total lysates were analyzed by Western blotting (W) with anti-HIS and anti-ERBB4 (sc-283). R697L disrupts the SH2 domain of VAV3; the 1-PH construct lacks the SH2 domain. *B*, COS-7 cells were transfected with ERBB4 ICD and WT or mutant MYC-HIS-tagged VAV3 constructs and analyzed as in *A*. *C*, COS-7 cells were transfected with constructs encoding WT or kinase-dead K751R ERBB4 and MYC-HIS-tagged VAV3. Lysates were immunoprecipitated with anti-ERBB4 (HFR-1). Immunoprecipitation samples and total lysates were analyzed by Western blotting with anti-MYC (2272) and anti-ERBB4 (E200). *D*, COS-7 cells were transfected with constructs encoding WT or mutant ERBB4 and MYC-HIS-tagged VAV3 and analyzed as in *C*.

ERBB4 antibody (Fig. 4). Western blotting analyses of the coprecipitates indicated that besides VAV3, ERBB4 also interacted with ectopically expressed VAV1 and VAV2 (Fig. 4).

ERBB4 stimulates tyrosine phosphorylation of VAV3

VAV GEF activity requires tyrosine phosphorylation of specific residues within the VAV activation domain (17). To assess the ability of ERBB4 to induce tyrosine phosphorylation of VAV3, *in vitro* kinase assays were carried out. COS-7 cells were transfected with empty vector or a vector encoding VAV3, and VAV3 was immunoprecipitated from the lysates. The precipitates were incubated without or with Strep-purified ERBB4 ICD and ATP and analyzed by Western blotting using a phosphotyrosine antibody. Tyrosine-phosphorylated VAV3 was

clearly detected as an ~100 kDa band in the sample containing ERBB4 ICD and ATP (Fig. 5A, lane 3). Autophosphorylated ERBB4 ICD was also detected as a band migrating at ~80 kDa (Fig. 5A, lanes 1 and 3).

To confirm the ability of ERBB4 to stimulate VAV3 phosphorylation, ERBB4 and VAV3 were coexpressed in COS-7 cells. VAV3 was immunoprecipitated from the cell lysates, and tyrosine phosphorylation was analyzed by Western blotting using a phosphotyrosine antibody (Fig. 5B). As in the *in vitro* kinase assay, a phosphotyrosine-reactive band of ~100 kDa was detected when both ERBB4 and VAV3 were expressed (Fig. 5B, lane 4).

To study whether ERBB4 could stimulate the phosphorylation of specific VAV3 tyrosines required for the GEF activity, a

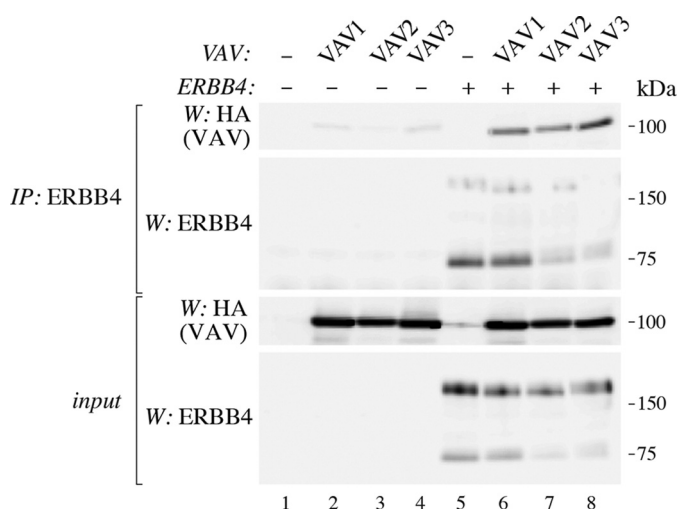


Figure 4. Interaction of ERBB4 with VAV1, VAV2, and VAV3. COS-7 cells were transfected with constructs encoding ERBB4 (JM-a CYT-2 isoform) and HA-tagged VAV1, VAV2, or VAV. Lysates were immunoprecipitated with anti-ERBB4 (sc-283). Immunoprecipitation (IP) samples and total lysates were analyzed by Western blotting (W) with anti-HA and anti-ERBB4 (sc-283).

VAV3 construct containing two tyrosine-to-phenylalanine mutations in conserved activation domain tyrosine residues (Tyr-160 and -173) was generated (17, 26). A third activation domain tyrosine residue (Tyr-164) was also mutated based on a prediction of likely phosphorylation sites by the Scansite tool (RRID:SCR_007026). A phosphotyrosine-reactive band representing tyrosine-phosphorylated WT VAV3 was again detected upon ERBB4 coexpression (Fig. 5C, lane 6). However, no VAV3 phosphorylation was detected when the triple tyrosine-to-phenylalanine mutant VAV3 was expressed instead of the WT, suggesting that ERBB4 could indeed stimulate the phosphorylation of the activation domain tyrosines (Fig. 5C, lane 8). Likewise, no phosphotyrosine-reactive band of VAV3 R697L was detected, confirming that physical interaction of ERBB4 and VAV3 was required for the ability of ERBB4 to stimulate the phosphorylation (Fig. 5C, lane 7).

To study the role of each of the three tyrosines in the VAV3 activation domain (Tyr-160, -164, and -173), single tyrosine-to-phenylalanine mutants were generated. Coexpression of the single and triple tyrosine-to-phenylalanine VAV3 mutants together with ERBB4 in COS-7 cells demonstrated that, whereas all of the 3 tyrosines contributed to VAV3 phosphorylation, Tyr-160 was the predominant site of ERBB4-dependent tyrosine phosphorylation (Fig. 5D).

To further characterize the role of the three VAV3 activation domain tyrosines for VAV3 signaling activity, the single and triple tyrosine-to-phenylalanine VAV3 mutants were coexpressed with ERBB4 in MCF-7 cells. To this end, we hypothesized that—if VAV3 activation by tyrosine phosphorylation was critical for its downstream signaling—the tyrosine-to-phenylalanine mutant VAV3 constructs should exhibit a dominant-negative effect on this signaling when overexpressed. As myosin light chain (MLC) is phosphorylated upon activation of the Rho family of GTPases (27, 28), phosphorylated MLC was used as an indirect indicator of VAV3 downstream signaling activity. Consistent with the observations of VAV3 phosphory-

lation (Fig. 5D), Y160F was the most efficient of the single mutants in reducing NRG-1-stimulated increase in MLC phosphorylation, whereas overexpression of the triple mutant Y160F/Y164F/Y173F abolished the effect (Fig. 5E).

These results indicate that ERBB4 stimulates tyrosine phosphorylation of VAV3 and that Tyr-160 is the major tyrosine residue phosphorylated by ERBB4. The ability of ERBB4 to induce the phosphorylation of VAV3 tyrosines required for its activation and the necessity of these tyrosines for NRG-1-stimulated phosphorylation of MLC suggests that ERBB4 can also activate cell signaling via VAV3.

VAV3 is a novel effector of ERBB4-mediated migration

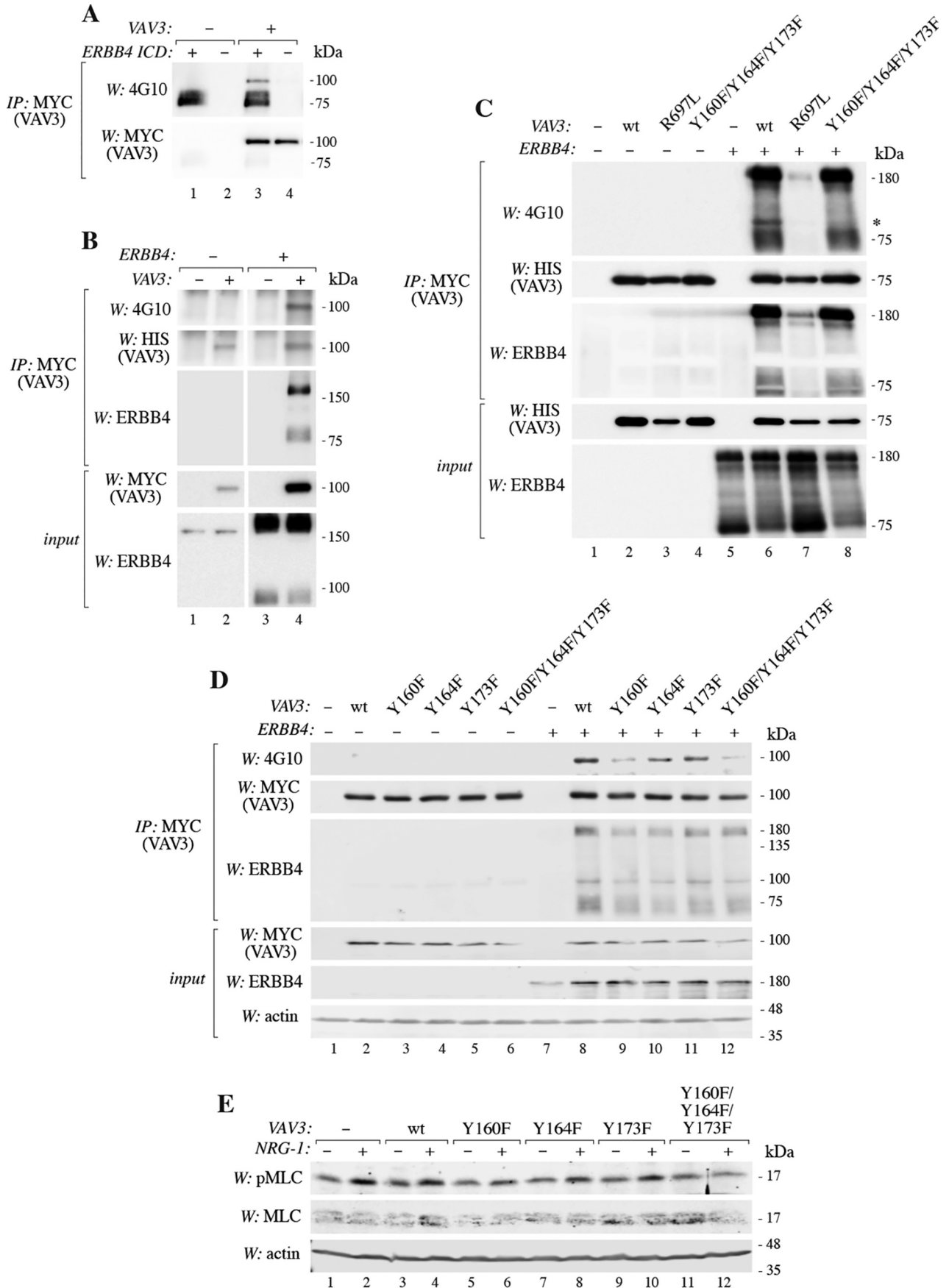
VAV3 functions as GEF for Rho GTPases, which regulate cytoskeletal dynamics and thus modulate cell motility (17). ERBB4 signaling promotes the migration of different cell types, including breast cancer cells (29–31), where ERBB4-VAV3 interaction was identified (Fig. 1C and Fig. S1). To address the role of VAV3 in ERBB4 signaling, fibroblast and breast cancer cell models of ERBB4-stimulated migration were used.

NIH 3T3-7d mouse fibroblast transfectants stably expressing the JM-b CYT-1 isoform of ERBB4, in a background with endogenous expression of both VAV2 and VAV3 (Fig. S3A), readily migrated toward the ERBB4 ligand NRG-1 in Transwell migration assays (Fig. 6, A–C), as described previously (10). Overexpression of dominant-negative VAV3 mutant construct, which encodes the SH2 and SH3 domains critical for mediating interactions with phosphotyrosines but not the catalytic GEF domain, resulted in reduced migration toward NRG-1 (Fig. 6, A–C). However, dominant-negative VAV3 mutant had no significant effect on the migration of 3T3 fibroblasts toward 1% fetal calf serum (Fig. 6, B and C).

To further characterize the functional significance of ERBB4-VAV3 signaling, migration of MCF-7 breast cancer cells was analyzed. MCF-7 cells express both ERBB4 and VAV3 endogenously (Fig. 6D and Fig. S3B) and have previously been used as a model of ERBB4-stimulated migration (30, 31). Knockdown of VAV3 with two independent shRNA constructs reduced the migration of MCF-7 cells in the absence of ligand stimulation (Fig. 6, D–F). NRG-1 significantly stimulated the migration of MCF-7 cells, and also ligand-induced migration was reduced upon knockdown of VAV3 (Fig. 6, E and F). ERBB4 silencing with shRNA or treatment of the cells with the ERBB tyrosine kinase inhibitor afatinib also reduced ligand-induced migration of MCF-7 cells (Fig. S4), confirming a functional role for ERBB4 in NRG-1-stimulated migration in the MCF-7 cell context.

Because all of the three VAV3 activation domain tyrosines (Tyr-160, -164, and -173) contributed to ERBB4-mediated VAV3 phosphorylation and NRG-1-stimulated VAV3 signaling activity (Fig. 5, D and E), the role of VAV3 activation in NRG-1-stimulated migration was further addressed. As our pMLC data (Fig. 5E) demonstrated that overexpression of the mutant VAV3 constructs was sufficient to functionally affect VAV3 downstream signaling in the MCF-7 cell background—consistent with a dominant-negative effect—the same overexpression approach was undertaken to address the effects on

ERBB4-VAV3 interaction



motility. Indeed, MCF-7 cells overexpressing the triple mutant Y160F/Y164F/Y173F VAV3 demonstrated a significantly impaired migratory response to NRG-1, as compared with cells overexpressing WT VAV3 (Fig. 6G). Taken together, these data indicate that ERBB4-VAV3 signaling regulates the migration of fibroblasts and breast cancer cells.

Discussion

Signaling cascades activated by ERBB4 receptor tyrosine kinase regulate cellular proliferation, differentiation, migration, and survival. ERBB4 signaling is involved in embryogenesis and homeostasis of adult tissues, but also in human pathologies including cancer (8, 9). Here, to discover novel molecular components of ERBB4 signaling, ERBB4-associating proteins in breast cancer cells were analyzed by MS. VAV3, a GEF for Rho GTPases, was identified as a novel ERBB4-associating protein. The ERBB4-VAV3 interaction depended on the SH2 domain of VAV3, intrinsic tyrosine kinase activity of ERBB4, and ERBB4 tyrosines 1022 and 1162. We also provide evidence indicating that VAV3 is a substrate for ERBB4-stimulated tyrosine phosphorylation and that VAV3 is required for efficient ERBB4-stimulated migration.

Both common and isoform-specific signaling mechanisms and functions of ERBB4 have been described (8). In agreement, our MS analysis identified both shared and specific interaction partners of ERBB4 cytoplasmic isoforms, including VAV3 as a novel CYT-2-associating protein. However, VAV3 also interacted with transiently expressed ERBB4 CYT-1 in coimmunoprecipitation experiments, and dominant-negative VAV3 inhibited CYT-1-stimulated migration. As ERBB4-VAV3 interaction requires tyrosine phosphorylation of ERBB4, differences in relative phosphorylation level of CYT-1 *versus* CYT-2 in different experimental conditions may explain these partially conflicting results. Coimmunoprecipitation of ERBB4 and VAV3 was carried out in experimental conditions where both isoforms are highly phosphorylated (12), and when equally phosphorylated (data not shown), both interacted with VAV3. Intriguingly, previous studies have described higher autokinase activity and tyrosine phosphorylation level of CYT-2 compared with CYT-1 (11, 12). Such difference in phosphorylation level could explain copurification of VAV3 with CYT-2, but not with CYT-1, in MS experiments. Again, due to the lack of antibodies specific to cytoplasmic ERBB4 isoforms, the relative phosphorylation level of endogenous CYT-1 and CYT-2 has not been analyzed, and the possibility of the CYT-2 isoform as a primary interaction partner of VAV3 in an endogenous setting cannot be excluded.

In addition to VAV3, ERBB4 also interacted with ectopically expressed VAV1 and VAV2. Due to significant similarity between the SH2 domains of different VAV proteins (26), it is likely that the interactions between ERBB4 and VAV1 and VAV2 are SH2-mediated, similar to the ERBB4-VAV3 interaction. The level of functional redundancy among the three VAV proteins is poorly understood, but VAV proteins appear to have partially overlapping functions (17). However, VAV family members have different expression patterns. Whereas VAV1 is primarily detected in cells of hematopoietic origin, VAV2 and VAV3 are expressed more broadly in both normal and cancer tissues, including many of the same tissues that express ERBB4 (RRID:SCR_018794 (8, 17, 32)).

EGFR, a closely related ERBB family member, also interacts with and stimulates tyrosine phosphorylation of VAV proteins (19, 22, 33). Two EGFR tyrosine residues (Tyr-1016 and -1172) have been described to mediate the EGFR-VAV2 interaction (22). Both of these residues are conserved in ERBB4 (EGFR Tyr-1061 and -1172 corresponding to ERBB4 Tyr-1022 and -1258, respectively), but of these two, only ERBB4 Tyr-1022 was necessary for the ERBB4-VAV3 interaction. As shown here for ERBB4 and VAV3, EGFR stimulates the phosphorylation of tyrosines within the VAV2 activation domain (22), which is required to release the VAV autoinhibited structure, thus allowing the GEF activity to occur (17). Mechanistically, the GEF function of VAV2 in EGF-stimulated cells appears to require PI3K activity even though VAV2 tyrosine phosphorylation is EGF- but not PI3K-dependent (22). It is currently unknown whether a similar mechanism regulates the signaling downstream of ERBB4-stimulated tyrosine phosphorylation of VAV3.

VAV proteins function as GEFs for Rho GTPases, which regulate cytoskeletal dynamics and thus modulate cell motility (17). In agreement, we showed that VAV3 activity is involved in the ERBB4-stimulated migration of fibroblasts and breast cancer cells. Previously, ERBB4 has been shown to mediate cell migration by direct coupling to PI3K (10). However, this signaling mechanism is limited to the ERBB4 CYT-1 isoform, as CYT-2 lacks the binding site for the P85 subunit of PI3K and does not mediate PI3K-dependent responses, including migration (Fig. 1, A and C (5, 10)). Our data, defining VAV GEFs as effectors of ERBB4 tyrosine kinase activity, thus describes a novel signaling mechanism that broadens the migration-promoting function of ERBB4 to comprise the CYT-2 isoform.

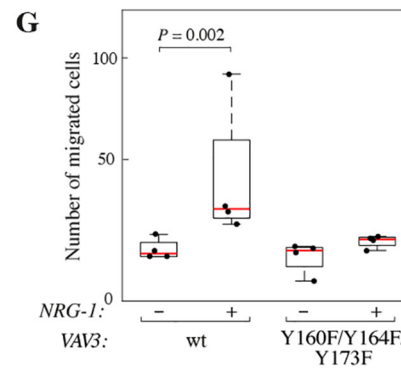
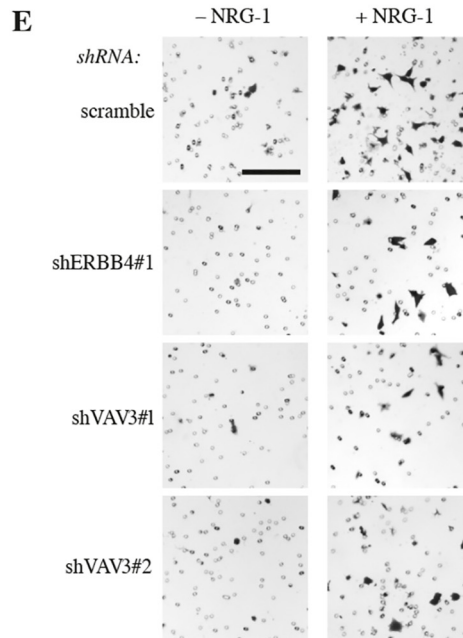
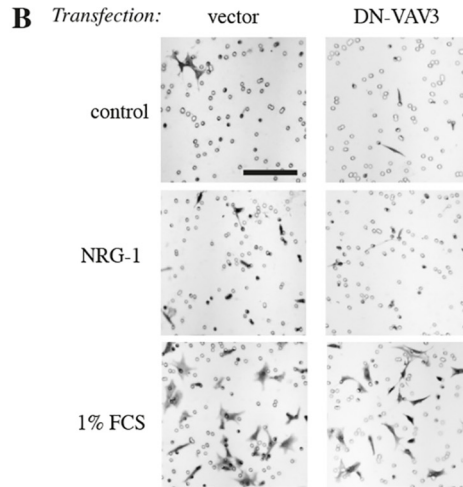
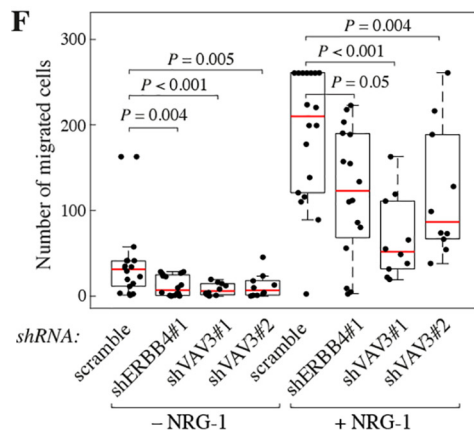
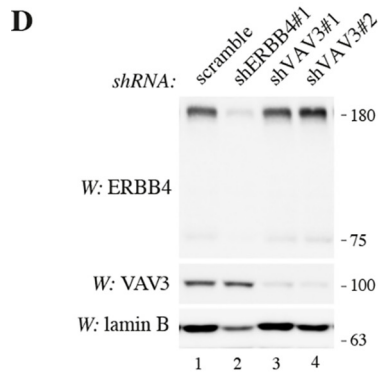
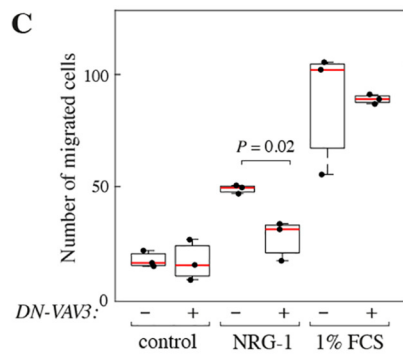
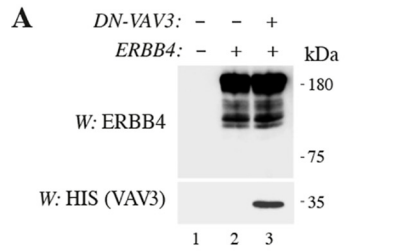
Both VAV2 and VAV3 have been reported to promote tumorigenesis and lung metastasis in a mouse model of breast cancer (34). Notably, the expression of VAV3 is markedly increased in human breast cancer when compared with

Figure 5. Phosphorylation of VAV3. A, lysates from COS-7 cells expressing MYC-HIS-tagged VAV3 were immunoprecipitated (IP) with anti-MYC (9E10), and precipitates were incubated without or with ERBB4 ICD (CYT-2 isoform, including the kinase domain) in the presence of ATP. Samples were analyzed by Western blotting (W) with anti-phosphotyrosine 4G10 and anti-MYC (9E10). B, COS-7 cells were transfected with ERBB4 (JM-a CYT-2 isoform) and MYC-HIS-tagged VAV3. Lysates were immunoprecipitated with anti-MYC (9E10), and samples were analyzed by Western with anti-phosphotyrosine 4G10, anti-HIS, and anti-ERBB4 (sc-283). Total lysates were analyzed by Western with anti-MYC (9E10) and anti-ERBB4 (sc-283). C, COS-7 cells were transfected with ERBB4 (JM-a CYT-2 isoform) and WT or mutant MYC-HIS-tagged VAV3. Lysates were immunoprecipitated with anti-MYC (9E10), and samples were analyzed by Western with anti-phosphotyrosine 4G10, anti-HIS, and anti-ERBB4 (E200). Total lysates were analyzed by Western blotting with anti-HIS and anti-ERBB4 (E200). R697L disrupts the SH2 domain of VAV3; Tyr-160, -164, and -173 are predicted phosphorylation sites of VAV3. D, lysates from COS-7 cells expressing ERBB4 (JM-a CYT-2 isoform) and WT or mutant MYC-HIS-tagged VAV3 were immunoprecipitated with anti-MYC (9E10) and analyzed by Western blotting with anti-phosphotyrosine 4G10, anti-MYC (9E10), and anti-ERBB4 (E200). Total lysates were analyzed by Western blotting with anti-MYC (9E10) and anti-ERBB4 (E200), and loading was controlled with anti-actin. E, MCF-7 cells expressing ERBB4 (JM-a CYT-2 isoform) and WT or mutant MYC-HIS-tagged VAV3 were stimulated with 50 ng/ml NRG-1 for 10 min. Lysates were analyzed by Western blotting with anti-phospho-MLC, anti-MLC, and anti-actin.

ERBB4-VAV3 interaction

normal breast tissue (RRID:SCR_018794 (32, 34)), whereas the expression of *VAV2* appears similar in both normal and cancer tissues (RRID:SCR_018794 (32, 34)). Increased *VAV3* expression is detected particularly in the estrogen receptor- and progesterone receptor-positive breast cancer (31, 33), a

subtype where *ERBB4* is also expressed (34–36). Importantly, in estrogen receptor-positive breast cancer treated with tamoxifen, high *VAV3* expression is associated with worse outcomes compared with low *VAV3* expression (37, 38). It is thus interesting to speculate whether the *ERBB4*-*VAV3*



signaling pathway promotes cancer cell migration and metastasis in breast cancer and whether drugs targeting ERBB4 (39, 40) could also limit VAV3 activity and metastasis.

In conclusion, we have demonstrated that VAV GEFs are novel effectors of ERBB4 signaling activity. Our data provide new understanding of molecular mechanisms underlying the ERBB4-regulated cellular processes. Finally, our findings describe a novel signaling pathway relevant for cancer cell migration.

Experimental procedures

Cell culture and transfections

COS-7, NIH 3T3-7d, and HEK 293T cells were cultured in Dulbecco's modified Eagle's medium, and MCF-7 cells were cultured in RPMI 1640. Both media were supplemented with 10% fetal calf serum (Biowest), 2 mM L-glutamine (Lonza), and 50 units/ml penicillin-streptomycin solution (Lonza). COS-7, NIH 3T3-7d, HEK 293T, and MCF-7 cells were transiently transfected with expression plasmids using FuGENE6 transfection reagent (Promega) or Lipofectamine2000 (Invitrogen) according to the manufacturer's protocol. To generate MCF-7 cell lines with stable expression, cells were selected with 500 μ g/ml G418 (Geneticin, Calbiochem).

Plasmids

The following expression plasmids have been described previously: pcDNA3.1hygro(+)-ERBB4JM-aCYT-2-HA, pcDNA3.1hygro(+)-ERBB4JM-aCYT-2-Myc, and pcDNA3.1hygro(+)-ERBB4ICD2-HA (11) and pcDNA3.1hygro(+)-ERBB4JM-aCYT-2-K751R-HA (41). pEF4myc/His-VAV3, pEF4myc/His-VAV3-R697L, and pEF4myc/His-VAV3- Δ C1-SH3B were gifts from Dr. Amnon Altman (23), and pC.HA-VAV1, pC.HA-VAV2, and pC.HA-VAV3 (Addgene plasmids 14553, 14554, and 14555) from Dr. Joan Brugge (7). Lentiviral packaging plasmids pMLDg/pRRE, pMD2.G, and pRSV-Rev (Addgene plasmids 12251, 12259, and 12253) were gifts from Dr. Didier Trono (42). C-terminal Strep-tags (WSHPQFEK) were added to pcDNA3.1neo(-)-ERBB4JM-aCYT-1 and pcDNA3.1neo(-)-ERBB4JM-aCYT-2 (15) by PCR to generate pcDNA3.1neo(-)-ERBB4JM-aCYT-1-Strep-tag and pcDNA3.1neo(-)-ERBB4JM-aCYT-2-Strep-tag.

To generate pcDNA3.1hygro(+)-ERBB4ICD2-Strep-tag, pcDNA3.1neo(-)-ERBB4JM-aCYT-2-Strep-tag was digested with XhoI and PmeI. The resulting 1140-bp DNA fragment, encoding for the C-terminal sequence of ERBB4 and with

the Strep-tag, was swapped to replace a 974-bp DNA fragment of pcDNA3.1hygro(+)-ERBB4ICD2, generated by digestion with XhoI and XbaI. Point mutations Y1022F, Y1162F, Y1202F, Y1208F, and Y1258F (amino acid numbers refer to the canonical ERBB4 JM-a CYT-1) were introduced to pcDNA3.1hygro(+)-ERBB4JM-aCYT-2-HA (15), and point mutations Y160F, Y164F, and Y173F were introduced to pEF4myc/His-VAV3 by site-directed mutagenesis.

To generate a dominant-negative form of VAV3, a DNA fragment encoding for the C-terminal part (containing amino acids 610-846; SH3-SH2-SH3 domains) of VAV3 was PCR-amplified with oligonucleotides (forward 5'-TTTTTTGAATT-CACGATGGCTCTGCATGAAGGACCCCTTTAC-3' and reverse 5'-TTTTTTAGCGGCCGCTTCATCTTCTTCCACATATGTGG-3') using pEF4myc/His-VAV3 as a template. The PCR fragment was digested with EcoRI and NotI and ligated into the place of the WT VAV3 insert in pEF4myc/His-VAV3. All generated constructs were confirmed by sequencing.

Purification of strep-tagged ERBB4 and MS

To identify ERBB4-interacting proteins in MCF-7 cells, Strep-tagged ERBB4 JM-a CYT-1 and ERBB4 JM-a CYT-2 and the interacting proteins were purified using Strep-Tactin Superflow columns (IBA). The purified proteins were separated by SDS-PAGE and silver-stained. The proteomics facility of the Biomedical Research Centre of the University of British Columbia performed in-gel trypsin digestion of the gel bands, tandem MS (MS/MS) analysis, protein database searching, and data analysis. The protein bands of interest were excised from the gel, reduced, alkylated, and digested overnight with trypsin, as described previously (43). The resulting mixture of peptides were analyzed by LC-MS/MS on a linear ion trap FT-ICR (LTQ-FT, Thermo Fisher Scientific) mass spectrometer coupled to an Agilent 1100 Series nanoflow HPLC (Agilent) using a 15-cm-long, 75- μ m inner diameter fused silica column packed with 3- μ m particle size Reprosil-Pur C-18-AQ beads (Dr. Maisch GmbH) with gradient elution, which used 0.5% aqueous acetic acid as mobile phase A and 0.5% acetic acid and 80% acetonitrile in water as mobile phase B. The gradient elution at a flow rate of 0.2 μ l/min was performed by changing %B as follows: 0.0–10.0 min, 6%; 10.1–60.0 min, 6–30%; 60.1–80.0 min, 30–80%; 80.1–90 min, 80%; 90.1–100 min, 6% (at a flow rate of 0.6 μ l/min to recondition the column). The LTQ-FT acquired a full-range scan at 25,000 resolution from 350 to 1500 Thomson in the FT-ICR cell before MS/MS analysis of

Figure 6. Role of VAV3 in ERBB4-dependent migration. A, NIH3T3-7d cells stably expressing ERBB4 (JM-b CYT-1 isoform) were transfected without or with a construct encoding MYC-HIS-tagged dominant-negative VAV3 construct (DN-VAV3). Expression of ERBB4 and VAV3 was analyzed by Western blotting (W) with anti-ERBB4 (sc-283) and anti-HIS. B, NIH3T3 transfectants were plated in Transwell cell culture inserts with or without 25 ng/ml NRG-1 or 1% fetal calf serum in the bottom well and allowed to migrate for 8 h before fixation and crystal violet staining. Representative images of cells migrated through the Transwell membrane are shown. Bar, 100 μ m. C, quantification of migrated cells. Data from three experiments are presented as a box plot, with horizontal lines indicating the median, boxes indicating the second and third quartile, and whiskers indicating the minimum and maximum values of the distribution. Individual data points are indicated as dots. For statistical testing, negative binomial regression analysis was used. The p values were Benjamini-Hochberg corrected for multiple testing error. D, MCF-7 cells stably expressing scrambled control shRNA or shRNAs targeting ERBB4 or VAV3 were analyzed for ERBB4 and VAV3 expression by Western with anti-ERBB4 (E200) and anti-VAV3. Anti-lamin B was used to control loading. E, MCF-7 cells stably expressing the indicated shRNAs were plated in Transwell cell culture inserts with 0 or 10 ng/ml NRG-1 in the bottom well. The cells were allowed to migrate for 8 h and analyzed as in B. Bar, 100 μ m. F, quantification of migrated cells. Data from 10–18 experiments are presented as a box plot with statistical analysis as in C, except that the whiskers indicate 1.5 \times interquartile range. G, quantification of migrated MCF-7 cells expressing WT or Y160F/Y164F/Y173F mutant VAV3. Migration was analyzed in the presence or absence of 10 ng/ml NRG-1 as in E. Data from four experiments are presented as a box plot with statistical analysis as in C.

ERBB4-VAV3 interaction

the top three ions in the LTQ (minimum intensity = 500 counts) was performed. A mass window for precursor ion selection of 1.0 and the normalized collision energy of 35 were applied. Selected ions were then excluded from MS/MS for the next 180 s. Singly charged ions were also excluded.

Acquired raw data were converted to Mascot input file using DTASuperCharge (2006-05-18, part of the MSQuant open source project) and searched against the SwissProt database (version 50.0, May 30, 2006) using the Mascot search engine. Searches were performed with a 20-ppm precursor mass tolerance and 0.5-Da fragment ion mass tolerance. Trypsin was selected as a protease and one missed cleavage was allowed. Allowed modifications included cysteine carbamidomethylation (+57.021 Da) as a static modification and methionine oxidation (+15.995 Da) as a variable modification. Expected value threshold of 0.01 was used to filter peptide spectral matches.

A minimum of two peptides was required to identify each protein. The specificity of the interactions was controlled by comparing the ERBB4-copurifying proteins to the proteins identified in vector control purifications.

Targeted proteomics

MCF-7 cells were serum-starved overnight and stimulated with 10 ng/ml NRG-1 β (R&D Biosystems) for 15 min. Cells were lysed and precleared with 50 μ l of Protein G-Sepharose (GE Healthcare). ERBB4 antibody (E200, Abcam) was incubated with Protein G magnetic beads (Millipore) for 1 h at room temperature followed by cross-linking antibodies to beads with 3 mM BS3 cross-linker (Thermo Scientific) for 30 min. The cross-linking reaction was quenched with 50 mM Tris, pH 7.4, and beads were washed three times with 0.2% Tween 20 in PBS. The precleared lysates were incubated with the ERBB4 antibody-bound magnetic beads overnight at 4 °C. The beads were washed seven times with 0.2% Tween 20 in PBS with 500 mM NaCl, one time with PBS, and two times with Milli-Q water. Bound proteins were eluted, reduced, and alkylated with 8 M urea, 5 mM tris(2-carboxyethyl)phosphine, 10 mM chloroacetamide, 100 mM Tris, pH 8.5, and 150 mM NaCl in 50 °C for 30 min. Eluted samples were digested with 1:100 (w/v) trypsin (Thermo Fisher Scientific) using a modified single-pot solid-phase-enhanced sample preparation (SP3) method (44) overnight at 37 °C. Following digestion, the reactions were quenched with 10% formic acid at a final concentration of ~1.0% (pH ~2) and dried by vacuum centrifugation (Heto Laboratory).

MS analysis was performed at the Turku Proteomics Facility at Turku Bioscience (University of Turku and Åbo Akademi University). Dried peptide samples were resuspended in 0.1% formic acid and analyzed on an Easy-nLC 1200 liquid chromatography system coupled to an Orbitrap Lumos Fusion instrument (Thermo Fisher Scientific) equipped with a nanoelectrospray source. Peptides were loaded on an in-house packed 100 μ m \times 2-cm precolumn packed with ReproSil-Pur 5- μ m 200-Å C18-AQ beads (Dr. Maisch) using 0.1% formic acid in water (buffer A) and separated by reverse phase chromatography on a 75 μ m \times 15-cm analytical column packed with ReproSil-Pur 5- μ m 200-Å C18-AQ beads (Dr. Maisch). All separations were

performed using a 40-min gradient at a flow rate of 300 nl/min. The gradient ranged from 6% buffer B (80% acetonitrile in 0.1% formic acid) to 36% buffer B in 30 min. Buffer B concentration was ramped up to 100% in 5 min, and 100% buffer B was run 5 min for washout.

VAV3 peptides for targeted proteomics were selected using an online parallel reaction monitor (PRM) method designer Picky (45) with default parameters, except miscleaved peptides were allowed, and the maximal number of features monitored in parallel was set to 31. A scheduled PRM method was used to simultaneously target all selected VAV3 peptides. The Orbitrap Lumos Fusion instrument was operated as follows. Targeted MS/MS spectra were acquired with a resolution of 30,000, automatic gain control target of $5e^4$, isolation window of m/z 1.6, maximum injection time set at 54 ms, and normalized collision energy = 27.

Acquired raw data were analyzed with Skyline (46), version 20.1.1.83, to identify peptides and quantify peak intensities. The ratio of peak areas was used to compare the relative abundance of peptides. The human protein database (Uniprot, September 9, 2019) was used as the background proteome. Spectra for selected VAV3 peptides were predicted using ProSight (47). After trial samples, the four best-scoring peptides (dotp values >0.8) were selected for further analysis.

Preparation of cell lysates and Western blotting

To prepare lysates for Western blotting, cells were washed with PBS; lysed in lysis buffer (1% Triton X-100, 10 mM Tris-Cl, pH 7.4, 150 mM NaCl, 1 mM EDTA, 5 mM NaF, 10 μ g/ml aprotinin, 10 μ g/ml leupeptin, 1 mM Na₃VO₄, 2 mM PMSF, and 10 mM Na₄P₂O₇); and centrifuged at 16,000 $\times g$ for 10 min. Protein concentration of the supernatants was measured by a Bradford protein assay (Bio-Rad). Equal amounts of samples were denatured by heating at 95 °C for 5 min in SDS-PAGE loading buffer. The samples were separated by SDS-PAGE and transferred to nitrocellulose membranes. Membranes were incubated with antibodies indicated in the figures. Signals were detected using enhanced chemiluminescence (Advansta) or using the Odyssey CLx imaging system (LI-COR). Lysates were prepared from 2–7 independent experiments for each Western and coimmunoprecipitation analysis.

Coimmunoprecipitation of ERBB4 and VAV3

COS-7 cells were transiently transfected with expression plasmids and lysed 24 h after transfection. Aliquots of lysates corresponding to 400–600 μ g of total protein were precleared with 30 μ l of Protein G-agarose (Santa Cruz Biotechnology) or Protein G-Sepharose at 4 °C for 1 h. Immunoprecipitation was carried out using antibodies recognizing ERBB4 (HFR-1 (Abcam) or sc-283 (Santa Cruz Biotechnology) or E200) or MYC (catalog no. 2272 (Cell Signaling Technology) or 9E10 (Invitrogen)) and 30 μ l of Protein G-agarose at 4 °C overnight. The beads were washed four times with 1 ml of lysis buffer and heated at 95 °C for 5 min in SDS-PAGE loading buffer to elute bound proteins. Precipitates were analyzed by Western blotting using anti-ERBB4 (E200 or sc-283), anti-HA (3F10, Roche Applied Science), anti-MYC (catalog no. 2272 (Cell Signaling

Technology) or 9E10), or anti-HIS (H1029, Sigma–Aldrich) antibodies as indicated in the figures.

Analysis of VAV3 tyrosine phosphorylation

For the *in vitro* kinase assay, ERBB4 CYT-2-Strep-tag was expressed in HEK 293T cells, affinity-purified using Strep-tactin (IBA), and eluted by desthiobiotin (IBA). MYC-HIS-tagged VAV3 was expressed in COS-7 cells. The cells were lysed in kinase assay lysis buffer (10% glycerol, 1% Triton X-100, 20 mM Hepes, pH 7.5, 50 mM NaCl, 10 μ g/ml aprotinin, 10 μ g/ml leupeptin, 2 mM PMSF), and lysates were subjected to immunoprecipitation using anti-MYC antibody (9E10). The samples were washed three times with kinase assay lysis buffer and twice with kinase assay buffer (5% glycerol, 20 mM Hepes, pH 7.7, 50 mM NaCl, 20 mM MgCl₂, 3 mM MnCl₂, 10 μ g/ml aprotinin, 10 μ g/ml leupeptin, 2 mM PMSF) and incubated in kinase assay buffer with 10 μ M ATP for 15 min at 25 °C in the presence or absence of 10 ng of ERBB4 CYT-2-Strep-tag. The samples were analyzed for tyrosine phosphorylation by Western blotting using anti-phosphotyrosine antibody (4G10, Upstate). VAV3 expression was controlled by Western blotting using anti-MYC antibody (9E10).

To analyze VAV3 tyrosine phosphorylation in COS-7 transfectants, cells were serum-starved overnight and lysed. VAV3 was immunoprecipitated using anti-MYC (9E10) antibody, and the precipitates were analyzed by Western blotting with phosphotyrosine antibody (4G10). The expression of ERBB4 was controlled by Western blotting using anti-ERBB4 (sc-283 or E200) and VAV3 immunoprecipitation with anti-MYC (9E10) or anti-HIS antibodies. Loading was controlled with anti-actin (A5441, Sigma–Aldrich).

Analysis of MLC phosphorylation

To analyze the role of VAV3 tyrosine phosphorylation in Rho-signaling pathway activation, MCF-7 cell transfectants were serum-starved overnight, stimulated with 50 ng/ml NRG-1 for 10 min, and lysed. Lysates were analyzed with anti-phospho-MLC (ab2480, Abcam) and anti-MLC (catalog no. 3674, Cell Signaling Technology). Loading was controlled with anti-actin (A5441).

Generation of cell lines with stable VAV3 or ERBB4 knockdown

Stable VAV3 and ERBB4 shRNA cell lines were generated using Mission shRNA lentiviruses (shVAV3#1, TRCN0000047702; shVAV3#2, TRCN0000047699; shERBB4#1, TRCN0000001411; shERBB4#2, TRCN0000039688; Sigma–Aldrich). Scramble shRNA (a gift from David Sabatini; Addgene plasmid 1864 (48)) was used as a control. For lentivirus production, plasmids encoding shRNAs were transfected into HEK 293T cells together with virus-packaging plasmids (pMLDg/pRRE, pMD2.G, and pRSV-Rev). Lentivirus-containing supernatants were harvested 48 h after transfection, filtered, and stored at –80 °C. MCF-7 cells were infected for 8 h with viral supernatants at multiplicity of infection of 1 in the presence of 8 μ g/ml Polybrene (Sigma–Aldrich). To generate stable cell lines, infected cells were selected with 1 μ g/ml puromycin (Life Technologies, Inc.). Knockdown efficacy of VAV3 and ERBB4 were determined by Western blotting using anti-VAV3 (catalog

no. 2398, Cell Signaling Technology) and anti-ERBB4 (E200) antibodies. Loading was controlled using Lamin B (sc-6217; Santa Cruz Biotechnology, Inc.) antibody.

Cell migration assay

NIH 3T3-7d cells stably expressing ERBB4 JM-b CYT-1 (clone b1.amg; described previously (5, 49)) were transiently transfected with empty vector or dominant-negative VAV3. Twenty-four hours after transfection, the cells were plated in Transwell inserts (8- μ m pore size; BD Falcon) in culture medium without serum. The bottom well was supplemented with 0 or 25 ng/ml NRG-1 or 1% fetal calf serum. The cells were allowed to migrate for 8 h, fixed with 4% paraformaldehyde, and stained with 0.2% crystal violet dissolved in 10% ethanol. After removing the nonmigrated cells in the upper chamber, each Transwell membrane was imaged for six randomly selected fields, and the number of migrated cells was counted. Negative binomial regression analysis was used to calculate the *p* values from the median number of migrated cells in each experiment. The *p* values were Benjamini–Hochberg corrected for multiple testing error.

Parental MCF-7 cells, MCF-7 cells stably expressing shRNAs, or MCF-7 cells transiently expressing MYC-HIS-tagged VAV3 constructs were plated in Transwell inserts in culture medium with 1% fetal calf serum. The bottom well was supplemented with 0 or 10 ng/ml NRG-1 and 0, 10, or 100 nM afatinib (Boehringer Ingelheim). The cells were allowed to migrate for 8 h and analyzed as described above from the total number of migrated cells from four randomly selected fields. The total number of migrated cells from shRNA-treated cells was normalized to the maximum number of migrated cells per cell batch to adjust for variance arising from cells cultured at different times. The statistical analysis was conducted as described above.

Data availability

The targeted MS proteomics data have been deposited to the ProteomeXchange Consortium via the PRIDE (50) partner repository with the data set identifier PXD019430. All remaining data are contained within the article.

Acknowledgments—We thank Minna Santanen, Mika Savisalo, and Maria Tuominen for skillful technical assistance and Dr. Ilkka Paa-tero for the expression and purification of ICD2-Strep-tag.

Author contributions—V. K. O. and J. A. M. M. validation; V. K. O., A. M. K., P. K., J. A. M. M., M. K., D. T., S. L., J. K., and A. T. P. investigation; V. K. O., P. K., J. A. M. M., and K. E. visualization; V. K. O., A. M. K., P. K., and J. A. M. M. methodology; V. K. O., A. M. K., P. K., and K. E. writing—original draft; V. K. O., A. M. K., and K. E. project administration; V. K. O., A. M. K., J. A. M. M., M. K., D. T., K. V., S. L., J. K., A. T. P., K. J. K., and K. E. writing—review and editing; A. M. K., D. T., A. T. P., K. J. K., and K. E. conceptualization; J. A. M. M. data curation; K. V. formal analysis; J. K. resources; K. J. K. and K. E. supervision; K. E. funding acquisition.

ERBB4-VAV3 interaction

Funding and additional information—This study has been supported by Academy of Finland (274728, 316796), the Cancer Foundation of Finland, and the Turku University Central Hospital.

Conflict of interest—K. E. has research agreements with Boehringer Ingelheim and Puma Biotechnology and ownership interest in Abomics, Novo Nordisk, Orion, and Roche.

Abbreviations—The abbreviations used are: ERBB, v-erb-b avian erythroblastic leukemia viral oncogene homolog; EGFR, epidermal growth factor receptor; GEF, guanine nucleotide exchange factor; VAV3, Vav guanine nucleotide exchange factor 3; VAV1, Vav guanine nucleotide exchange factor 1; VAV2, Vav guanine nucleotide exchange factor 2; shRNA, short hairpin RNA; RTK, receptor tyrosine kinase; EGF, epidermal growth factor; PI3K, phosphoinositol 3-kinase; JM, juxtamembrane; CYT, cytoplasmic; TACE, tumor necrosis factor- α -converting enzyme; ICD, intracellular domain; SH2, Src homology 2 domain; P85A, phosphatidylinositol-3-kinase regulatory subunit α ; NRG, neuregulin; MYC, MYC proto-oncogene; HIS, histidine; MLC, myosin light chain; SH3, Src homology 3 domain; FT-ICR, Fourier-transform ion cyclotron resonance; LTQ, linear trap quadrupole; SP3, single-pot solid-phase-enhanced sample preparation; PRM, parallel reaction monitor; PMSF, phenylmethylsulfonyl fluoride.

References

1. Yarden, Y., and Pines, G. (2012) The ERBB network: at last, cancer therapy meets systems biology. *Nat. Rev. Cancer* **12**, 553–563 [CrossRef Medline](#)
2. Elenius, K., Corfas, G., Paul, S., Choi, C. J., Rio, C., Plowman, G. D., and Klagsbrun, M. (1997) A novel juxtamembrane domain isoform of HER4/Erbb4: isoform-specific tissue distribution and differential processing in response to phorbol ester. *J. Biol. Chem.* **272**, 26761–26768 [CrossRef Medline](#)
3. Rio, C., Buxbaum, J. D., Peschon, J. J., and Corfas, G. (2000) Tumor necrosis factor-converting enzyme is required for cleavage of erbB4/HER4. *J. Biol. Chem.* **275**, 10379–10387 [CrossRef Medline](#)
4. Ni, C.-Y., Murphy, M. P., Golde, T. E., and Carpenter, G. (2001) γ -Secretase cleavage and nuclear localization of ErbB-4 receptor tyrosine kinase. *Science* **294**, 2179–2181 [CrossRef Medline](#)
5. Elenius, K., Choi, C. J., Paul, S., Santiestevan, E., Nishi, E., and Klagsbrun, M. (1999) Characterization of a naturally occurring ErbB4 isoform that does not bind or activate phosphatidylinositol 3-kinase. *Oncogene* **18**, 2607–2615 [CrossRef Medline](#)
6. Sundvall, M., Korhonen, A., Paatero, I., Gaudio, E., Melino, G., Croce, C. M., Aqeilan, R. I., and Elenius, K. (2008) Isoform-specific monoubiquitination, endocytosis, and degradation of alternatively spliced ErbB4 isoforms. *Proc. Natl. Acad. Sci. U. S. A.* **105**, 4162–4167 [CrossRef Medline](#)
7. Omerovic, J., Santangelo, L., Puggioni, E. M.-R., Marrocco, J., Dall'Armi, C., Palumbo, C., Belleudi, F., Di Marcotullio, L., Frati, L., Torrisi, M.-R., Cesareni, G., Gulino, A., and Alimandi, M. (2007) The E3 ligase Aip4/Itch ubiquitinates and targets ErbB-4 for degradation. *FASEB J.* **21**, 2849–2862 [CrossRef Medline](#)
8. Veikkolainen, V., Vaparanta, K., Halkilahti, K., Iljin, K., Sundvall, M., and Elenius, K. (2011) Function of ERBB4 is determined by alternative splicing. *Cell Cycle* **10**, 2647–2657 [CrossRef Medline](#)
9. Hollmén, M., and Elenius, K. (2010) Potential of ErbB4 antibodies for cancer therapy. *Future Oncol.* **6**, 37–53 [CrossRef Medline](#)
10. Kainulainen, V., Sundvall, M., Määttä, J. A., Santiestevan, E., Klagsbrun, M., and Elenius, K. (2000) A natural ErbB4 isoform that does not activate phosphoinositide 3-kinase mediates proliferation but not survival or chemotaxis. *J. Biol. Chem.* **275**, 8641–8649 [CrossRef Medline](#)
11. Määttä, J. A., Sundvall, M., Junttila, T. T., Peri, L., Laine, V. J. O., Isola, J., Egeblad, M., and Elenius, K. (2006) Proteolytic cleavage and phosphorylation of a tumor-associated ErbB4 isoform promote ligand-independent survival and cancer cell growth. *Mol. Biol. Cell* **17**, 67–79 [CrossRef Medline](#)
12. Sundvall, M., Peri, L., Määttä, J. A., Tvorogov, D., Paatero, I., Savisalo, M., Silvennoinen, O., Yarden, Y., and Elenius, K. (2007) Differential nuclear localization and kinase activity of alternative ErbB4 intracellular domains. *Oncogene* **26**, 6905–6914 [CrossRef Medline](#)
13. Sundvall, M., Korhonen, A., Vaparanta, K., Anckar, J., Halkilahti, K., Salah, Z., Aqeilan, R. I., Palvimo, J. J., Sistonen, L., and Elenius, K. (2012) Protein inhibitor of activated STAT3 (PIAS3) protein promotes SUMOylation and nuclear sequestration of the intracellular domain of ErbB4 protein. *J. Biol. Chem.* **287**, 23216–23226 [CrossRef Medline](#)
14. Linggi, B., and Carpenter, G. (2006) ErbB-4 s80 intracellular domain abrogates ETO2-dependent transcriptional repression. *J. Biol. Chem.* **281**, 25373–25380 [CrossRef Medline](#)
15. Merilahti, J. A. M., and Elenius, K. (2018) γ -Secretase-dependent signaling of receptor tyrosine kinases. *Oncogene* **38**, 151–163 [CrossRef Medline](#)
16. Gilmore-Hebert, M., Ramabhadran, R., and Stern, D. F. (2010) Interactions of ErbB4 and Kap1 connect the growth factor and DNA damage response pathways. *Mol. Cancer Res.* **8**, 1388–1398 [CrossRef Medline](#)
17. Bustelo, X. R. (2014) Vav family exchange factors: an integrated regulatory and functional view. *Small GTPases* **5**, 9–12 [CrossRef Medline](#)
18. Bustelo, X. R. (2018) RHO GTPases in cancer: known facts, open questions, and therapeutic challenges. *Biochem. Soc. Trans.* **46**, 741–760 [CrossRef Medline](#)
19. Pandey, A., Podtelejnikov, A. V., Blagoev, B., Bustelo, X. R., Mann, M., and Lodish, H. F. (2000) Analysis of receptor signaling pathways by mass spectrometry: identification of Vav-2 as a substrate of the epidermal and platelet-derived growth factor receptors. *Proc. Natl. Acad. Sci. U. S. A.* **97**, 179–184 [CrossRef Medline](#)
20. Schulze, W. X., Deng, L., and Mann, M. (2005) Phosphotyrosine interactome of the ErbB-receptor kinase family. *Mol. Syst. Biol.* **1**, 2005.0008 [CrossRef Medline](#)
21. Lemmon, M. A., and Schlessinger, J. (2010) Cell signaling by receptor tyrosine kinases. *Cell* **141**, 1117–1134 [CrossRef](#)
22. Tamás, P., Solti, Z., Bauer, P., Illés, A., Sipéki, S., Bauer, A., Faragó, A., Downward, J., and Buday, L. (2003) Mechanism of epidermal growth factor regulation of Vav2, a guanine nucleotide exchange factor for Rac. *J. Biol. Chem.* **278**, 5163–5171 [CrossRef Medline](#)
23. Charvet, C., Canonigo, A. J., Billadeau, D. D., and Altman, A. (2005) Membrane localization and function of Vav3 in T cells depend on its association with the adapter SLP-76. *J. Biol. Chem.* **280**, 15289–15299 [CrossRef Medline](#)
24. Kaushansky, A., Gordus, A., Budnik, B. A., Lane, W. S., Rush, J., and MacBeath, G. (2008) System-wide investigation of ErbB4 reveals 19 sites of Tyr phosphorylation that are unusually selective in their recruitment properties. *Chem. Biol.* **15**, 808–817 [CrossRef Medline](#)
25. Hause, R. J., Leung, K. K., Barkinge, J. L., Ciaccio, M. F., Chuu, C. P., and Jones, R. B. (2012) Comprehensive binary interaction mapping of SH2 domains via fluorescence polarization reveals novel functional diversification of ErbB receptors. *PLoS ONE* **7**, e44471 [CrossRef Medline](#)
26. Movilla, N., and Bustelo, X. R. (1999) Biological and regulatory properties of Vav-3, a new member of the Vav family of oncoproteins. *Mol. Cell Biol.* **19**, 7870–7885 [CrossRef Medline](#)
27. Amano, M., Ito, M., Kimura, K., Fukata, Y., Chihara, K., Nakano, T., Matsuura, Y., and Kaibuchi, K. (1996) Phosphorylation and activation of myosin by Rho-associated kinase (Rho-kinase). *J. Biol. Chem.* **271**, 20246–20249 [CrossRef Medline](#)
28. Watanabe, G., Saito, Y., Madaule, P., Ishizaki, T., Fujisawa, K., Morii, N., Mukai, H., Ono, Y., Kakizuka, A., and Narumiya, S. (1996) Protein kinase N (PKN) and PKN-related protein Rhophilin as targets of small GTPase Rho. *Science* **271**, 645–648 [CrossRef Medline](#)
29. Haskins, J. W., Nguyen, D. X., and Stern, D. F. (2014) Neuregulin 1-activated ERBB4 interacts with YAP to induce Hippo pathway target genes and promote cell migration. *Sci. Signal.* **7**, ra116–ra116 [CrossRef Medline](#)
30. Kiuchi, T., Ortiz-Zapater, E., Monypenny, J., Matthews, D. R., Nguyen, L. K., Barbeau, J., Coban, O., Lawler, K., Burford, B., Rolfe, D. J., De Rinaldis, E., Dafou, D., Simpson, M. A., Woodman, N., Pinder, S., et al. (2014)

- The ErbB4 CYT2 variant protects EGFR from ligand-induced degradation to enhance cancer cell motility. *Sci. Signal.* **7**, ra78–ra78 [CrossRef Medline](#)
31. Mill, C. P., Zordan, M. D., Rothenberg, S. M., Settleman, J., Leary, J. F., and Riese, D. J. (2011) ErbB2 is necessary for ErbB4 ligands to stimulate oncogenic activities in models of human breast cancer. *Genes Cancer* **2**, 792–804 [CrossRef Medline](#)
 32. Kilpinen, S., Autio, R., Ojala, K., Iljin, K., Bucher, E., Sara, H., Pisto, T., Saarela, M., Skotheim, R. I., Björkman, M., Mpindi, J.-P., Haapa-Paananen, S., Vainio, P., Edgren, H., Wolf, M., *et al.* (2008) Systematic bioinformatic analysis of expression levels of 17,330 human genes across 9,783 samples from 175 types of healthy and pathological tissues. *Genome Biol.* **9**, R139 [CrossRef Medline](#)
 33. Moores, S. L., Selfors, L. M., Fredericks, J., Breit, T., Fujikawa, K., Alt, F. W., Brugge, J. S., and Swat, W. (2000) Vav family proteins couple to diverse cell surface receptors. *Mol. Cell Biol.* **20**, 6364–6373 [CrossRef Medline](#)
 34. Citterio, C., Menacho-Márquez, M., García-Escudero, R., Larive, R. M., Barreiro, O., Sánchez-Madrid, F., Paramio, J. M., and Bustelo, X. R. (2012) The Rho exchange factors Vav2 and Vav3 control a lung metastasis-specific transcriptional program in breast cancer cells. *Sci. Signal.* **5**, ra71 [CrossRef Medline](#)
 35. Sundvall, M., Iljin, K., Kilpinen, S., Sara, H., Kallioniemi, O. P., and Elenius, K. (2008) Role of ErbB4 in breast cancer. *J. Mammary Gland Biol. Neoplasia* **13**, 259–268 [CrossRef Medline](#)
 36. Lee, K., Liu, Y., Mo, J. Q., Zhang, J., Dong, Z., and Lu, S. (2008) Vav3 oncogene activates estrogen receptor and its overexpression may be involved in human breast cancer. *BMC Cancer* **8**, 158 [CrossRef Medline](#)
 37. Aguilar, H., Urruticoechea, A., Halonen, P., Kiyotani, K., Mushiroda, T., Barril, X., Serra-Musach, J., Islam, A., Caizzi, L., Di Croce, L., Nevedomskaya, E., Zwart, W., Bostner, J., Karlsson, E., Pérez Tenorio, G., *et al.* (2014) VAV3 mediates resistance to breast cancer endocrine therapy. *Breast Cancer Res.* **16**, R53 [CrossRef Medline](#)
 38. Chen, X., Chen, S., Liu, X. A., Zhou, W., Bin, Ma, R. R., and Chen, L. (2015) Vav3 oncogene is upregulated and a poor prognostic factor in breast cancer patients. *Oncol. Lett.* **9**, 2143–2148 [CrossRef Medline](#)
 39. Solca, F., Dahl, G., Zoephel, A., Bader, G., Sanderson, M., Klein, C., Kraemer, O., Himmelsbach, F., Haaksmma, E., and Adolf, G. R. (2012) Target binding properties and cellular activity of afatinib (BIBW 2992), an irreversible ErbB family blocker. *J. Pharmacol. Exp. Ther.* **343**, 342–350 [CrossRef Medline](#)
 40. Modjtahedi, H., Cho, B. C., Michel, M. C., and Solca, F. (2014) A comprehensive review of the preclinical efficacy profile of the ErbB family blocker afatinib in cancer. *Naunyn Schmiedebergs Arch. Pharmacol.* **387**, 505–521 [CrossRef Medline](#)
 41. Tvorogov, D., Sundvall, M., Kurppa, K., Hollmén, M., Repo, S., Johnson, M. S., and Elenius, K. (2009) Somatic mutations of ErbB4: selective loss-of-function phenotype affecting signal transduction pathways in cancer. *J. Biol. Chem.* **284**, 5582–5591 [CrossRef Medline](#)
 42. Dull, T., Zufferey, R., Kelly, M., Mandel, R. J., Nguyen, M., Trono, D., and Naldini, L. (1998) A third-generation lentivirus vector with a conditional packaging system. *J. Virol.* **72**, 8463–8471 [CrossRef Medline](#)
 43. Shevchenko, A., Wilm, M., Vorm, O., and Mann, M. (1996) Mass spectrometric sequencing of proteins from silver-stained polyacrylamide gels. *Anal. Chem.* **68**, 850–858 [CrossRef Medline](#)
 44. Hughes, C. S., Moggridge, S., Müller, T., Sorensen, P. H., Morin, G. B., and Krijgsveld, J. (2019) Single-pot, solid-phase-enhanced sample preparation for proteomics experiments. *Nat. Protoc.* **14**, 68–85 [CrossRef Medline](#)
 45. Zuber, H., Kirchner, M., and Selbach, M. (2018) Picky: a simple online PRM and SRM method designer for targeted proteomics. *Nat. Methods* **15**, 156–157 [CrossRef Medline](#)
 46. MacLean, B., Tomazela, D. M., Shulman, N., Chambers, M., Finney, G. L., Frewen, B., Kern, R., Tabb, D. L., Liebler, D. C., and MacCoss, M. J. (2010) Skyline: an open source document editor for creating and analyzing targeted proteomics experiments. *Bioinformatics* **26**, 966–968 [CrossRef Medline](#)
 47. Gessulat, S., Schmidt, T., Zolg, D. P., Samaras, P., Schnatbaum, K., Zerweck, J., Knaute, T., Rechenberger, J., Delanghe, B., Huhmer, A., Reimer, U., Ehrlich, H. C., Aiche, S., Kuster, B., and Wilhelm, M. (2019) ProSIT: proteome-wide prediction of peptide tandem mass spectra by deep learning. *Nat. Methods* **16**, 509–518 [CrossRef Medline](#)
 48. Sarbassov, D. D., Guertin, D. A., Ali, S. M., and Sabatini, D. M. (2005) Phosphorylation and regulation of Akt/PKB by the rictor-mTOR complex. *Science* **307**, 1098–1101 [CrossRef Medline](#)
 49. Zhang, K., Sun, J., Liu, N., Wen, D., Chang, D., Thomason, A., and Yoshinaga, S. K. (1996) Transformation of NIH 3T3 Cells by HER3 or HER4 receptors requires the presence of HER1 or HER2. *J. Biol. Chem.* **271**, 3884–3890 [Medline](#)
 50. Perez-Riverol, Y., Csordas, A., Bai, J., Bernal-Llinares, M., Hewapathirana, S., Kundu, D. J., Inuganti, A., Griss, J., Mayer, G., Eisenacher, M., Pérez, E., Uszkoreit, J., Pfeuffer, J., Sachsenberg, T., Yilmaz, S., *et al.* (2019) The PRIDE database and related tools and resources in 2019: improving support for quantification data. *Nucleic Acids Res.* **47**, D442–D450 [CrossRef Medline](#)
 51. Junttila, T. T., Laato, M., Vahlberg, T., Söderström, K.-O., Visakorpi, T., Isola, J., and Elenius, K. (2003) Identification of patients with transitional cell carcinoma of the bladder overexpressing ErbB2, ErbB3, or specific ErbB4 isoforms: real-time reverse transcription-PCR analysis in estimation of ErbB receptor status from cancer patients. *Clin. Cancer Res.* **9**, 5346–5357 [Medline](#)